Eur. Phys. J. B **8**, 511–523 (1999)

THE EUROPEAN PHYSICAL JOURNAL B

EDP Sciences

Suppression of antiferromagnetic correlations by quenched dipole-type impurities

V. Cherepanov, I.Ya. Korenblit, A. Aharony[a], and O. Entin-Wohlman

School of Physics and Astronomy, Raymond and Beverly Sackler Faculty of Exact Sciences, Tel Aviv University, Tel Aviv 69978, Israel

Received 22 October 1998

Abstract. The effects of quenched dipole moments on a two-dimensional Heisenberg antiferromagnet are found exactly, by applying the renormalization group to the appropriate classical non-linear sigma model. Such dipole moments represent random fields with power law correlations. At low temperatures, they also represent the long range effects of quenched random strong ferromagnetic bonds on the antiferromagnetic correlation length, ξ_{2D}, of a two-dimensional Heisenberg antiferromagnet. It is found that the antiferromagnetic long range order is destroyed for any non-zero concentration, x, of the dipolar defects, even at zero temperature. Below a line $T \propto x$, where T is the temperature, ξ_{2D} is independent of T, and decreases exponentially with x. At higher temperatures, it decays exponentially with ρ_s^{eff}/T, with an effective stiffness constant ρ_s^{eff}, which decreases with increasing x/T. The latter behavior is the same as for annealed dipole moments, and we use our quenched results to interpolate between the two types of averaging for the problem of ferromagnetic bonds in an antiferromagnet. The results are used to estimate the three-dimensional Néel temperature of a lamellar system with weakly coupled planes, which decays linearly with x at small concentrations, and drops precipitously at a critical concentration. These predictions are shown to reproduce successfully several of the prominent features of experiments on slightly doped copper oxides.

PACS. 75.10.-b General theory and models of magnetic ordering – 75.10.Nr Spin-glass and other random models – 75.50.Ee Antiferromagnetics

1 Introduction

Consider an isotropic Heisenberg antiferromagnet, with a concentration x of quenched random nearest neighbor ferromagnetic (FM) bonds, called impurities. These bonds compete with the antiferromagnetic (AFM) order (which results from the concentration $(1-x)$ of the AFM bonds), and introduce frustration into the problem. If the FM exchange on the "impurity" bonds is sufficiently strong, then the two spins at the end of each such bond prefer energetically to be parallel to each other, and perpendicular to the background AFM staggered moment. The staggered moments on the other sites then cant in this perpendicular direction, and at large distance this canting angle decays with distance r as $1/r^{d-1}$ in d dimensions, similarly to the decay of magnetic moments in the presence of a magnetic dipole [1,2]. This follows [1] from a mapping of the low temperature equations for the spin configuration at the minimal energy onto the Laplace equation (see also below, following Eq. (4)). The present paper presents a renormalization group (RG) analysis of the AFM correlations in the presence of such quenched dipoles. As we show, this complex random problem is exactly renormalizable in two dimensions (2D), allowing a detailed study of the dependence of the 2D AFM correlation length ξ_{2D} on T and on x. This also allows an ϵ-expansion in $d = 2+\epsilon$ dimensions. The three-dimensional Néel temperature $T_N(x)$ of lamellar systems is then estimated by a model of weakly coupled planes.

The description of FM bonds in a doped antiferromagnet by dipoles requires several assumptions, which will be discussed in detail below. In particular, at high temperature T the "dipolar" moments which describe the dopant bonds may fluctuate, turning this aspect of the problem into one which requires a combined annealed and quenched averaging. Indeed, Glazman and Ioselevich (GI) [3] studied this problem in its annealed limit, and calculated ξ_{2D} to leading order in x/T (See also Ref. [4]) Although the locations $\mathbf{r}_\ell$ of the dipole-like impurities are randomly *quenched*, each impurity involves an effective dipole moment $\mathbf{m}(\mathbf{r}_\ell)$ which is still free to reach *annealed* equilibrium in the presence of all the other dipoles. As we show below, the effective dipoles develop dipole-dipole interactions among them. Since the locations of the dipoles are random, one expects them to behave like a dipole glass. However, unlike the dipole glass, where the interactions are fixed, the interactions among the dipoles are mediated by the AFM spin background, whose behavior also depends on temperature, concentration and configuration

[a] e-mail: aharony@post.tau.ac.il

of the dipole moments. In the absence of a simple systematic way to handle such a combined quenched-annealed problem, GI stopped their explicit calculations at the low-x expansion. Here we argue that at sufficiently low T the dipole moments, which interact via randomly quenched dipole-dipole interactions, either freeze in a random spin glassy way or at least develop very long range spin-glassy correlations [5,6]. Assuming that the range of these correlations is much larger than that of the AFM correlations, this justifies treating these moments as quenched. Indeed, this assumption is then confirmed by our calculations, which yield a *finite* AFM correlation length at all T and finite x. Our calculations are thus complementary to those of GI: theirs apply at low x, and ours apply at low T. The actual fitting of data from doped antiferromagnets should involve some interpolation between the annealed and quenched limits. To leading order in x/T, the annealed and quenched calculations give the same results. Therefore, our quenched results supply a good interpolation over the whole range. Indeed, we show below that our theory is consistent with data from doped cuprates, which may be described at low doping as having localized ferromagnetic bonds in a lamellar antiferromagnet [7].

Another major motivation of our study of quenched random dipoles concerns the fact that, as we show below, such dipoles are coupled to the gradient of the order parameter, and therefore they are equivalent to correlated random fields, whose correlations in momentum space are proportional to the square of the momentum. Such fields lower the critical dimensions of the random field $\mathcal{N}$-component spin model by 2, from 6 to 4 for the upper critical dimension, and from 4 to 2 for the lower one. In reference [8] this has been established for the limit $\mathcal{N} \to \infty$. Here we show that the lower critical dimension is shifted down from $d = 4$ to $d = 2$, for all $\mathcal{N} > 2$. As a result, both the temperature and the variance of the random dipole moments (which is proportional to the concentration, x) are marginal (in the RG sense) at $d = 2$, allowing for an analytical solution of the recursion relations. This marginality of the randomness is related to the 2D infrared divergence of the Villain canted states [1]. Within the one-loop approximation, we obtain an exact expression for the exponential part of the 2D correlation length, which remains finite at all non-zero x.

We describe the system by the reduced Hamiltonian (*i.e.*, the Hamiltonian divided by the temperature T)

$$\mathcal{H} = \mathcal{H}_{pure} + \mathcal{H}_{int}, \tag{1}$$

where $\mathcal{H}_{pure}$ is the classical non-linear sigma model (NLσM) for the pure (non-random) system, representing the long wave length Hamiltonian related to the fluctuations of the unit vector $\mathbf{n}(\mathbf{r})$ of antiferromagnetism,

$$\mathcal{H}_{pure} = \frac{1}{2t} \int d\mathbf{r} \sum_{i,\mu} (\partial_i n_\mu)^2, \quad t = T/\rho_s. \tag{2}$$

Here $i = 1, ..., d$ and $\mu = 1, ..., \mathcal{N}$ run over the spatial Cartesian components and over the spin components, respectively, ρ_s is the stiffness constant and $\partial_i \equiv \partial/\partial x_i$. This Hamiltonian is known to give an excellent description of the undoped antiferromagnet, both theoretically [9] and experimentally [10]. The usual treatment of this model assumes long range order in some direction, and then treats the $\mathcal{N} - 1$ transverse spin components (called σ_μ) perturbatively. The success of this description results from the fact that, although the problem involves quantum spin fluctuations, these can be integrated out at any finite T, causing only a renormalization of ρ_s.

$\mathcal{H}_{int}$ is constructed [3] to reproduce the dipolar effects at long distances: Denoting by $\mathbf{a}(\mathbf{r}_\ell)$ the unit vector directed along the doped bond at $\mathbf{r}_\ell$, and by $M\mathbf{m}(\mathbf{r}_\ell)$ the corresponding dipole moment (where $\mathbf{m}(\mathbf{r}_\ell)$ is a unit vector giving the direction of the dipole, and M is its magnitude),

$$\mathcal{H}_{int} = \frac{1}{t} \int d\mathbf{r} \sum_i \mathbf{f}_i(\mathbf{r}) \cdot \partial_i \mathbf{n}, \tag{3}$$

with

$$\mathbf{f}_i(\mathbf{r}) = M \sum_\ell \delta(\mathbf{r} - \mathbf{r}_\ell) a_i(\mathbf{r}_\ell) \mathbf{m}(\mathbf{r}_\ell). \tag{4}$$

Note that since $\mathbf{n}$ is a unit vector, $\partial_i \mathbf{n}$ is perpendicular to $\mathbf{n}$ and hence $\mathcal{H}_{int}$ contains only the $\mathcal{N} - 1$ components of the $\mathcal{N}$-component vector $\mathbf{f}_i$ which are transverse to $\mathbf{n}$. However, since the vector $\mathbf{n}$ varies with $\mathbf{r}$, all the components of $\mathbf{m}$ may enter at the end. To see the dipolar nature of $\mathcal{H}_{int}$, note that for a single impurity at the origin, $\mathcal{H}$ is minimized when the Fourier transform of n_μ solves the Laplace equation

$$q^2 n_\mu(\mathbf{q}) = M m_\mu i \mathbf{a} \cdot \mathbf{q}, \tag{5}$$

with the solution $\mathbf{n}(\mathbf{r}) = \mathbf{n}_0 + \delta\mathbf{n}(\mathbf{r})$, where $\delta\mathbf{n}(\mathbf{r}) = -M\mathbf{m}\mathbf{a} \cdot \mathbf{r}/(2\pi r^2)$, just as for a dipole in 2D. A similar Laplace equation appears when one looks for the minimum energy of a Heisenberg system at low temperatures, when the angles between neighboring spins are small [1].

As stated, GI treated the variables $\mathbf{m}$ as annealed. Here we treat all the variables $\mathbf{r}_\ell$, $\mathbf{a}(\mathbf{r}_\ell)$, and $\mathbf{m}(\mathbf{r}_\ell)$ as quenched. Denoting quenched averages by [...], we write

$$\begin{aligned} \big[\mathbf{a}(\mathbf{r})\big] &= 0, \\ \big[m_\mu(\mathbf{r})\big] &= 0, \\ \big[a_i(\mathbf{r}) a_j(\mathbf{r}')\big] &= \delta_{ij} \delta(\mathbf{r} - \mathbf{r}') x/d, \\ \big[m_\mu(\mathbf{r}) m_\nu(\mathbf{r}')\big] &= Q \delta_{\mu\nu} \delta(\mathbf{r} - \mathbf{r}'), \end{aligned} \tag{6}$$

so that $[f_{i\mu}] = 0$ and

$$\big[f_{i\mu}(\mathbf{r}) f_{j\nu}(\mathbf{r}')\big] = \lambda \delta_{\mu\nu} \delta_{ij} \delta(\mathbf{r} - \mathbf{r}'), \tag{7}$$

with

$$\lambda = M^2 Q x/d \equiv A x, \tag{8}$$

where $A = \mathcal{O}(1)$. At low T one expects $Q \approx 1/\mathcal{N}$.

One can see now that $\mathcal{H}_{int}$ represents random fields with quenched correlations: Fourier transforming the variables in equation (3), $\mathcal{H}_{int}$ can be written in the form

$$\mathcal{H}_{int} = \frac{1}{(2\pi)^d t} \int d\mathbf{k} \sum_{\mu} h_\mu(\mathbf{k}) n_\mu(-\mathbf{k}), \tag{9}$$

with the random field $\mathbf{h}(\mathbf{k})$,

$$h_\mu(\mathbf{k}) = i \sum_j k_j \int d\mathbf{r} f_{j\mu}(\mathbf{r}) e^{i\mathbf{k}\cdot\mathbf{r}}, \tag{10}$$

which has quenched correlations

$$\left[h_\mu(\mathbf{k}) h^*_\nu(\mathbf{k}')\right] = \lambda k^2 \delta_{\mu\nu} \delta(\mathbf{k} - \mathbf{k}'). \tag{11}$$

Such correlations shift the critical dimension of the random field Heisenberg problem down to 2. A heuristic way to show this follows Imry and Ma [11] in assuming an ordered state and considering the transverse spin fluctuations, $\mathcal{M}^\perp(\mathbf{r})$. In momentum space, one has $\mathcal{M}^\perp(\mathbf{q}) = G^\perp(\mathbf{q}) h^\perp(\mathbf{q})$, with $G^\perp(\mathbf{q}) \sim 1/q^2$, where $h^\perp(\mathbf{q})$ denotes the transverse random field. Thus

$$\left[\mathcal{M}^\perp(\mathbf{r}) \mathcal{M}^\perp(\mathbf{r}')\right] = \left(\frac{1}{2\pi}\right)^{2d} \int d^d q d^d q' G^\perp(\mathbf{q}) G^\perp(\mathbf{q}') \times \left[h^\perp(\mathbf{q}) h^\perp(\mathbf{q}')\right] e^{i(\mathbf{q}\cdot\mathbf{r} + \mathbf{q}'\cdot\mathbf{r}')}. \tag{12}$$

For $\left[h_\mu(\mathbf{q}) h_\nu(\mathbf{q}')\right] \propto \delta_{\mu\nu} q^\theta \delta(\mathbf{q} + \mathbf{q}')$, this integral diverges for $d < 4 - \theta$, implying that the assumption of long range order is invalid. This identifies the lower critical dimension as $d_\ell = 4 - \theta$, and for our case, $d_\ell = 2$. The calculations below support this picture. In addition to giving an exact solution for the problem at hand, we note that the present formalism might also be used as a starting point for a double expansion, in ϵ and in $2-\theta$, aiming at other random field problems.

The conventional method to treat the NLσM expands the order parameter unit vector $\mathbf{n}$ about a spatially uniform ordered state [12,13]. Using replicas to handle the quenched randomness we have found that this approach generated local random fields, which seem to break the symmetries of the original model. Similar problems were found for other problems near 4D, where they required a resummation of the perturbation expansion [14]. Uncorrelated random fields were also generated in a renormalization group analysis of correlated random fields for the Ising model [15]. We suspect that those fields are also artifacts of the method used. We hope that the present study will reopen a discussion of these problems, which are important for our understanding of the analysis of correlated random systems. In our case, the problems may have come either from the replicas or from the assumption of a spatially uniform state. Such a state does not exist when there is some local freezing of the moments in random directions (as happens in the random case discussed here). We avoid both of these by going back to the original RG approach by Polyakov [16], and by treating the randomness without replicas. In 2D, this allows us to obtain ξ_{2D} for all values of $\rho_s x/T$.

We show that the quenched dipoles suppress the antiferromagnetic correlations, so that the correlation length is a decreasing function of $\rho_s x/T$, remaining finite at any non-zero x, even at $T = 0$. This implies the destruction of the antiferromagnetic long range order in 2D for any concentration. As x increases, $\xi_{2D}(T = 0)$ decays exponentially, representing the sizes of the Imry-Ma domains for this system.

In order to compare the results of our model with experiments, which are usually performed on quasi-2D, or lamellar, systems of weakly coupled planes, we consider the 3D ordering of such a system by using the relation $\alpha \xi_{2D}^2 \sim 1$. Here, α represents either the interplane coupling, that is the relative interplane exchange, $J_\perp/J \sim J_\perp/2\pi\rho_s$, or the in-plane relative spin anisotropy (in the presence of which even an infinitesimal coupling suffices to yield 3D ordering). Although it is not expected to give the correct 3D critical behavior, this procedure proved to give excellent results for the 3D Néel temperature in the pure case [10]. This "mean field" procedure is also justified by an RG argument: to linear order in α, the RG recursion relation for α is $\alpha' = e^{2\ell}\alpha$, where e^ℓ is the length rescale factor. After ℓ iterations of the RG the effective coupling between planes involves renormalized spins, contained in the area $e^{2\ell}$ of the renormalized cell. A 3D behavior is expected when this effective coupling becomes comparable to 1. As we show in Appendix B, similar results for the phase diagram are also found from integrating the RG recursion relations in $d = 2 + \epsilon$ dimensions.

The outline of the paper is as follows. Section 2 discusses the RG procedure, and Section 3 describes the RG recursion relations for the quenched averaging. The 2D recursion relations are then solved in Section 4, and the resulting ξ_{2D} is used for estimating the 3D phase transition line $T_N(x)$ in Section 5. Section 6 then contains a discussion of the alternative annealed averaging. The results are compared with experiments on doped cuprates in Section 7, and discussed in Section 8. Details of the calculations and extensions to $d = 2 + \epsilon$ are given in the Appendices.

2 The renormalization group procedure

Following the RG approach of Polyakov [16,17], we decompose $\mathbf{n}(\mathbf{r})$ into a slowly varying part, given by the unit vector $\tilde{\mathbf{n}}(\mathbf{r})$, and $\mathcal{N} - 1$ fast variables $\phi_\mu(\mathbf{r})$ (replacing the "usual" σ_μ's), such that

$$\mathbf{n}(\mathbf{r}) = \tilde{\mathbf{n}}(\mathbf{r}) \sqrt{1 - \phi^2(\mathbf{r})} + \sum_{\mu=1}^{\mathcal{N}-1} \phi_\mu(\mathbf{r}) \mathbf{e}_\mu(\mathbf{r}),$$
$$\phi^2(\mathbf{r}) = \sum_{\mu=1}^{\mathcal{N}-1} \phi_\mu^2(\mathbf{r}). \tag{13}$$

The unit vectors $\tilde{\mathbf{n}}(\mathbf{r})$ and $\mathbf{e}_\mu(\mathbf{r})$, $\mu = 1, ..., \mathcal{N} - 1$, form an orthonormal basis. The Fourier transform of the fast

variables ϕ_μ,

$$\phi_\mu(\mathbf{r}) = (2\pi)^{-d} \int d\mathbf{q} e^{i\mathbf{q}\mathbf{r}} \phi_\mu(\mathbf{q}), \tag{14}$$

is restricted to wave vectors $\mathbf{q}$ in the range $b^{-1} \leq q \leq 1$. The upper bound is the inverse of the microscopic length (which is measured in units of the lattice constant), and b is the length rescale factor for the renormalization procedure. These q values are to be integrated out. After the iteration the correlation length ξ is renormalized into ξ/b.

The Hamiltonian $\mathcal{H}$ requires the derivatives of $\mathbf{n}(\mathbf{r})$. Using the relations $\tilde{\mathbf{n}}\cdot\partial_i\tilde{\mathbf{n}} = 0$, $\tilde{\mathbf{n}}\cdot\mathbf{e}_\mu = 0$, and $\mathbf{e}_\mu\cdot\mathbf{e}_\nu = \delta_{\mu\nu}$, we set

$$\partial_i\tilde{\mathbf{n}} = \sum_{\mu=1}^{\mathcal{N}-1} B_i^\mu \mathbf{e}_\mu, \ \partial_i\mathbf{e}_\mu = \sum_{\nu=1}^{\mathcal{N}-1} A_i^{\mu\nu}\mathbf{e}_\nu - B_i^\mu\tilde{\mathbf{n}}, \tag{15}$$

where $A_i^{\nu\mu} = \mathbf{e}_\mu\cdot\partial_i\mathbf{e}_\nu = -A_i^{\mu\nu}$. Then we find

$$\partial_i\mathbf{n} = \tilde{\mathbf{n}}\left\{\partial_i\sqrt{1-\phi^2} - \sum_{\mu=1}^{\mathcal{N}-1} B_i^\mu\phi_\mu\right\} + \sum_{\mu=1}^{\mathcal{N}-1}\mathbf{e}_\mu\left\{\partial_i\phi_\mu + B_i^\mu\sqrt{1-\phi^2} + \sum_{\nu=1}^{\mathcal{N}-1} A_i^{\nu\mu}\phi_\nu\right\}. \tag{16}$$

We show in Appendix A that the functions $A_i^{\mu\nu}$, which give the first derivatives of the base vectors $\mathbf{e}_\mu$, can be eliminated by a suitable gauge transformation when one ignores higher order derivatives [16,18]. Therefore, these are omitted in the following.

In terms of the new variables, the Hamiltonian $\mathcal{H}$, to order ϕ_μ^2, reads

$$\mathcal{H} = \mathcal{H}_0 + \mathcal{H}_1 + \mathcal{H}_2 + \mathcal{H}_3 + \mathcal{H}_4, \tag{17}$$

with

$$\mathcal{H}_0 = \frac{1}{2t}\int d\mathbf{r}\sum_{i\mu}\left\{\left(B_i^\mu(\mathbf{r})\right)^2 + \left(\partial_i\phi_\mu(\mathbf{r})\right)^2\right\}, \tag{18}$$

$$\mathcal{H}_1 = \frac{1}{t}\int d\mathbf{r}\sum_{i\mu} B_i^\mu(\mathbf{r}) g_i^\mu(\mathbf{r}), \tag{19}$$

$$\mathcal{H}_2 = \frac{1}{2t}\int d\mathbf{r}\sum_{i\nu\mu} B_i^\mu(\mathbf{r})B_i^\nu(\mathbf{r})\left\{\phi_\mu(\mathbf{r})\phi_\nu(\mathbf{r}) - \delta_{\mu\nu}\phi^2(\mathbf{r})\right\}, \tag{20}$$

$$\mathcal{H}_3 = -\frac{1}{t}\int d\mathbf{r}\sum_{i\mu} B_i^\mu(\mathbf{r})\left\{u_i(\mathbf{r})\phi_\mu(\mathbf{r}) + \frac{1}{2}g_i^\mu(\mathbf{r})\phi^2\right\}, \tag{21}$$

and

$$\mathcal{H}_4 = \frac{1}{t}\int d\mathbf{r}\sum_{i\mu}\left\{g_i^\mu(\mathbf{r})\partial_i\phi_\mu(\mathbf{r}) - \frac{1}{2}u_i(\mathbf{r})\partial_i\phi_\mu^2(\mathbf{r})\right\}. \tag{22}$$

Here we have introduced the notations

$$u_i(\mathbf{r}) = \tilde{\mathbf{n}}(\mathbf{r})\cdot\mathbf{f}_i(\mathbf{r}), \quad g_i^\mu(\mathbf{r}) = \mathbf{e}_\mu(\mathbf{r})\cdot\mathbf{f}_i(\mathbf{r}), \tag{23}$$

for the longitudinal and transverse components, respectively, of $\mathbf{f}_i$ in the new variables. Indeed, equation (19) represents the bare form of $\mathcal{H}_{int}$ in this system. In $\mathcal{H}_0$ the slow variables, B_i^μ, are separated from the fast ones ϕ_μ. [One should notice that $(\partial_i n_\mu)^2$ also yields the contribution $(1/t)\int d\mathbf{r}\sum_{i\mu} B_i^\mu\partial_i\phi_\mu$. However, this term vanishes upon Fourier transforming, as ϕ_μ pertains to the large q portion of the Brillouin zone, while the slow variables B_i^μ belong to the small q values, $q \leq b^{-1}$.] The Hamiltonians $\mathcal{H}_2$, $\mathcal{H}_3$, and $\mathcal{H}_4$, of order $\mathcal{O}(B^2)$, $\mathcal{O}(B^1)$, and $\mathcal{O}(B^0)$, respectively, will be treated in perturbation theory.

3 Renormalization group equations

The first step in deriving the recursion relations involves integration over the fast variables ϕ_μ. This requires the Green's functions,

$$\begin{aligned}\langle\phi_\mu(\mathbf{r})\phi_\nu(\mathbf{r}')\rangle &= \delta_{\mu\nu}G(\mathbf{r}-\mathbf{r}'),\\ G(\mathbf{r}) &= (2\pi)^{-d}\int_{b^{-1}\leq q\leq 1} d\mathbf{q}e^{i\mathbf{q}\cdot\mathbf{r}}\hat{G}(q),\\ \hat{G}(q) &= t/q^2,\end{aligned} \tag{24}$$

where $\langle ...\rangle$ denotes a thermal average with $\mathcal{H}_0$. As we shall see below, to leading order in $\epsilon = d-2$ we need $G(r)$ only at strictly 2D, where

$$G(0) = \frac{t}{2\pi}\ln b. \tag{25}$$

Hence $\langle\phi^2\rangle$ is small for $\ln b \ll 2\pi/t$. In practice, $G(r)$ is significantly different from zero only for $1 < r < b$, where it is approximately given by the 2D Coulomb interaction

$$G(r) \approx \frac{t}{2\pi}\ln\frac{b}{r}\cdot \tag{26}$$

We next turn to the perturbation expansion in $\mathcal{H}_2$, $\mathcal{H}_3$, and $\mathcal{H}_4$. The first order yields

$$\begin{aligned}\mathcal{H}^{(1)} &= \langle\mathcal{H}_2 + \mathcal{H}_3\rangle\\ &= \frac{1}{2t}\int d\mathbf{r}\sum_{i\mu}\left(B_i^\mu(\mathbf{r})\right)^2(2-\mathcal{N})G(0)\\ &\quad - \frac{1}{2t}\int d\mathbf{r}\sum_{i\mu} B_i^\mu(\mathbf{r})g_i^\mu(\mathbf{r})(\mathcal{N}-1)G(0).\end{aligned} \tag{27}$$

The first term here represents the leading order renormalization of $1/t$, as usual [13,16]. The second term, which is linear in B_i^μ, is similar to the initial $\mathcal{H}_{int}$, or to the equivalent equation (19). In fact, this term contributes to the renormalization of the transverse components of $\mathbf{f}_i$.

Higher order perturbations contain higher powers of ϕ, which yield higher powers of G and hence of t. In the following, we keep only leading powers of t. Neglecting

the terms involving products of two G's, the second order perturbation yields

$$\begin{aligned}\mathcal{H}^{(2)} &= -\frac{1}{2}\langle(\mathcal{H}_3+\mathcal{H}_4)^2\rangle \\ &= -\frac{1}{2t^2}\int d\mathbf{r}_1 d\mathbf{r}_2 \sum_{ij\mu} g_i^\mu(\mathbf{r}_1) g_j^\mu(\mathbf{r}_2)\partial_{1i}\partial_{2j}G(\mathbf{r}_{12}) \\ &+ \frac{1}{t^2}\int d\mathbf{r}_1 d\mathbf{r}_2 \sum_{ij\mu} B_i^\mu(\mathbf{r}_1) u_i(\mathbf{r}_1) g_j^\mu(\mathbf{r}_2)\partial_{2j}G(\mathbf{r}_{12}) \\ &- \frac{1}{2t^2}\int d\mathbf{r}_1 d\mathbf{r}_2 \sum_{ij\mu} B_i^\mu(\mathbf{r}_1) B_j^\mu(\mathbf{r}_2) u_i(\mathbf{r}_1) u_j(\mathbf{r}_2) G(\mathbf{r}_{12}), \\ \mathbf{r}_{12} &= \mathbf{r}_1 - \mathbf{r}_2. \end{aligned} \tag{28}$$

The first term here is B-independent. In principle, it gives rise to an interaction between the dipoles: Inserting $G(\mathbf{r})$ and the explicit expressions for g_i^μ (Eqs. (4, 23)) we rewrite this term in the form

$$\mathcal{H}_{dd} = \frac{1}{t}\sum_{k\ell} I_{k\ell}\mathbf{m}_\perp(\mathbf{r}_k)\cdot\mathbf{m}_\perp(\mathbf{r}_\ell), \tag{29}$$

where $\mathbf{m}_\perp(\mathbf{r}_\ell)$ is the component of the dipole moment at $\mathbf{r}_\ell$ which is perpendicular to $\tilde{\mathbf{n}}$. In $d=2$ one has

$$I_{k\ell} = \frac{1}{4\pi}M^2\frac{1}{r_{k\ell}^2} \times\left\{2\frac{\big(\mathbf{a}(\mathbf{r}_k)\cdot\mathbf{r}_{k\ell}\big)\big(\mathbf{a}(\mathbf{r}_\ell)\cdot\mathbf{r}_{k\ell}\big)}{r_{k\ell}^2} - \mathbf{a}(\mathbf{r}_k)\cdot\mathbf{a}(\mathbf{r}_\ell)\right\}, \tag{30}$$

with $r_{k\ell} < b$. Apart from trivial factors, this reproduces the effective dipole-dipole interaction found in reference [3]. There, equation (29) was used to integrate over the variables $\mathbf{m}_\perp$, treating them as annealed variables. In the present calculation we treat the dipoles as quenched, and therefore equation (29) simply represents a constant which is to be added to the energy. We return to this point in the following. The other two (B-dependent) terms in the second order perturbation Hamiltonian, equation (28), will contribute to the renormalization of the temperature and the variance of the dipolar quenched interaction.

Finally, the third order perturbation Hamiltonian, keeping terms up to order B^2, is

$$\mathcal{H}^{(3)} = \frac{1}{6}\langle\mathcal{H}_4^3\rangle + \frac{1}{2}\left(\langle\mathcal{H}_4^2\mathcal{H}_3\rangle + \langle\mathcal{H}_4\mathcal{H}_3^2\rangle + \langle\mathcal{H}_2\mathcal{H}_4^2\rangle\right). \tag{31}$$

Integrating out the variables ϕ, it is seen that the first term here is independent of B; it contributes further to the dipole-dipole interaction. The next term in (31) yields an expression linear in B,

$$\begin{aligned}\frac{1}{2}\langle\mathcal{H}_4^2\mathcal{H}_3\rangle = -\frac{1}{2t^3}\int d\mathbf{r}_1 d\mathbf{r}_2 d\mathbf{r}_3 \sum_{ijk}\sum_\mu B_i^\mu(\mathbf{r}_1) \\ \times\Big\{\sum_\nu g_i^\mu(\mathbf{r}_1) g_j^\nu(\mathbf{r}_2) g_k^\nu(\mathbf{r}_3)\partial_{2j}\partial_{3k}G(\mathbf{r}_{21})G(\mathbf{r}_{31}) \\ - 2u_i(\mathbf{r}_1) g_j^\mu(\mathbf{r}_2) u_k(\mathbf{r}_3)\partial_{2j}\partial_{3k}G(\mathbf{r}_{23})G(\mathbf{r}_{31})\Big\},\end{aligned} \tag{32}$$

which again contributes to $\mathcal{H}_{int}$, while the last term there gives a B^2 contribution

$$\begin{aligned}\frac{1}{2}\langle\mathcal{H}_4\mathcal{H}_3^2 + \mathcal{H}_2\mathcal{H}_4^2\rangle = \frac{1}{2t^3}\int d\mathbf{r}_1 d\mathbf{r}_2 d\mathbf{r}_3 \sum_{ijk}\sum_\mu \\ \times\Big\{-B_i^\mu(\mathbf{r}_1)B_i^\mu(\mathbf{r}_2)u_i(\mathbf{r}_1)u_j(\mathbf{r}_2)u_k(\mathbf{r}_3)\partial_{3k}G(\mathbf{r}_{13})G(\mathbf{r}_{23}) \\ + 2\sum_\nu B_i^\mu(\mathbf{r}_1)B_j^\nu(\mathbf{r}_2)u_i(\mathbf{r}_1)g_j^\nu(\mathbf{r}_2)g_k^\mu(\mathbf{r}_3)\partial_{3k}G(\mathbf{r}_{12})G(\mathbf{r}_{23}) \\ + \sum_\nu\big(B_i^\mu(\mathbf{r}_1)B_i^\nu(\mathbf{r}_1)g_j^\mu(\mathbf{r}_2)g_k^\nu(\mathbf{r}_3) \\ - B_i^\mu(\mathbf{r}_1)B_i^\mu(\mathbf{r}_1)g_j^\nu(\mathbf{r}_2)g_k^\nu(\mathbf{r}_3)\big)\partial_{2j}\partial_{3k}G(\mathbf{r}_{12})G(\mathbf{r}_{13})\Big\}.\end{aligned} \tag{33}$$

Except for the first term in equation (27), all the generated terms involve the longitudinal and transverse components of the vectors $\mathbf{f}_i$, u_i and g_i^μ, equation (23), which depend on the quenched random variables $\mathbf{r}_\ell$, $\mathbf{a}(\mathbf{r}_\ell)$, and $\mathbf{m}(\mathbf{r}_\ell)$. Using equation (7) we thus find

$$\begin{aligned}\big[g_i^\mu(\mathbf{r})g_j^\nu(\mathbf{r}')\big] &= \lambda\delta_{ij}\delta_{\mu\nu}\delta(\mathbf{r}-\mathbf{r}'), \\ \big[u_i(\mathbf{r})u_j(\mathbf{r}')\big] &= \lambda\delta_{ij}\delta(\mathbf{r}-\mathbf{r}'), \\ \big[u_i(\mathbf{r})g_j^\mu(\mathbf{r}')\big] &= 0.\end{aligned} \tag{34}$$

We now obtain the recursion relations of the RG. Consider first the quenched averages of the integrated Hamiltonians $\mathcal{H}^{(\ell)}, \ell = 1,2,3$. This will constitute the renormalization of $1/t$. Rescaling the lengths by b^{-1} and the slow derivatives $B_i^\mu(\mathbf{q})$ by b^{d-1}, the new temperature prefactor, multiplying the integral over $(B_i^\mu)^2$, obeys the RG equation

$$\frac{1}{t'} = b^{d-2}\left[\frac{1}{t} + \frac{2-\mathcal{N}}{2\pi}\ln b + \frac{1-\mathcal{N}}{2\pi}\frac{\lambda}{t}\ln b\right], \tag{35}$$

which is valid to first order in $\epsilon = d-2$, t and λ. To obtain this equation, we have used equations (34) and the relation

$$\sum_j\int d\mathbf{r}_2\big(\partial_{2j}G(\mathbf{r}_{12})\big)^2 = tG(0). \tag{36}$$

The terms in the Hamiltonian linear in B_i^μ remain as quenched random contributions. They renormalize $f_{i\mu}$ and yield a renormalization of its variance λ. To obtain the recursion relation for λ, we collect all terms linear in B and write them in the form

$$\frac{1}{t}\int d\mathbf{r}\sum_{i\mu} B_i^\mu(\mathbf{r})\Gamma_i^\mu(\mathbf{r}), \tag{37}$$

with

$$\Gamma_i^{\mu}(\mathbf{r}) = g_i^{\mu}(\mathbf{r})\left(1-\frac{1}{2}(\mathcal{N}-1)G(0)\right) + \frac{1}{t}\int d\mathbf{r}_1 \sum_j u_i(\mathbf{r})g_j^{\mu}(\mathbf{r}_1)\partial_{1j}G(\mathbf{r}-\mathbf{r}_1) - \frac{1}{2t^2}\int d\mathbf{r}_1 d\mathbf{r}_2 \sum_{jk} \Bigg\{\sum_{\nu} g_i^{\mu}(\mathbf{r})g_j^{\nu}(\mathbf{r}_1)g_k^{\nu}(\mathbf{r}_2)\partial_{1j}\partial_{2k}G(\mathbf{r}_1-\mathbf{r})G(\mathbf{r}_2-\mathbf{r}) - 2u_i(\mathbf{r})g_j^{\mu}(\mathbf{r}_1)u_k(\mathbf{r}_2)\partial_{1j}\partial_{2k}G(\mathbf{r}_1-\mathbf{r}_2)G(\mathbf{r}_2-\mathbf{r})\Bigg\}. \tag{38}$$

We then find the variance of $\Gamma_i^{\mu}(\mathbf{r})$ by the one-loop calculation, which to leading order, using equations (34), yields

$$\left[\Gamma_i^{\mu}(\mathbf{r})\Gamma_{i'}^{\mu'}(\mathbf{r}')\right] = \delta_{ii'}\delta_{\mu\mu'}\delta(\mathbf{r}-\mathbf{r}') \times \lambda\left(1-(\mathcal{N}-1)G(0)+\frac{\lambda}{t}(2-\mathcal{N})G(0)\right). \tag{39}$$

Hence, the recursion relation for λ is

$$\left(\frac{\lambda}{t^2}\right)' = b^{d-2}\frac{\lambda}{t^2}\left[1-\frac{t(\mathcal{N}-1)+\lambda(\mathcal{N}-2)}{2\pi}\ln b\right]. \tag{40}$$

One also needs to consider the fluctuations of the random terms around their quenched averages, as well as new terms, which were not included in the initial $\mathcal{H}$, but are generated by the renormalization procedure. However, these are irrelevant. Let us take as an example the last term in (28), which we may write as

$$\frac{1}{2t}\int d\mathbf{r}_1 d\mathbf{r}_2 \sum_{\mu ij} W_{ij}(\mathbf{r}_1\mathbf{r}_2)B_i^{\mu}(\mathbf{r}_1)B_j^{\mu}(\mathbf{r}_2). \tag{41}$$

Physically, this term describes a random interaction among the gradients of the order parameter $\mathbf{n}$, which are absent in the original problem. As the ensemble average contribution of this interaction has been analyzed above (see the last term in Eq. (35)), we need to consider here the deviation

$$\delta W_{ij}(\mathbf{r}_1\mathbf{r}_2) = -\frac{1}{t}\Big[u_i(\mathbf{r}_1)u_j(\mathbf{r}_2)-\lambda\delta_{ij}\delta(\mathbf{r}_1-\mathbf{r}_2)\Big]G(\mathbf{r}_{12}). \tag{42}$$

Using equations (34), it is easy to see that

$$[\delta W_{ij}(\mathbf{r}_1\mathbf{r}_2)\delta W_{i'j'}(\mathbf{r}_1'\mathbf{r}_2')] = \frac{\lambda^2}{t^2}\big[\delta_{ii'}\delta_{jj'}\delta(\mathbf{r}_1-\mathbf{r}_1')\delta(\mathbf{r}_2-\mathbf{r}_2') + \delta_{ij'}\delta_{ji'}\delta(\mathbf{r}_1-\mathbf{r}_2')\delta(\mathbf{r}_2-\mathbf{r}_1')\big]G(\mathbf{r}_{12})^2. \tag{43}$$

Since the range of $G(\mathbf{r})$ is of order b, the correlations among these generated W's are short range, and in practice the W's can be treated as uncorrelated, *i.e.*

$$[\delta W_{ij}(\mathbf{r}_1\mathbf{r}_2)\delta W_{i'j'}(\mathbf{r}_1'\mathbf{r}_2')] = \Delta\big[\delta_{ii'}\delta_{jj'}\delta(\mathbf{r}_1-\mathbf{r}_1')\delta(\mathbf{r}_2-\mathbf{r}_2') + \delta_{ij'}\delta_{ji'}\delta(\mathbf{r}_1-\mathbf{r}_2')\delta(\mathbf{r}_2-\mathbf{r}_1')\big]\delta(\mathbf{r}_{12}). \tag{44}$$

A simple power counting then shows that (W/t) scales as b^{2d-2}, W scales as b^d and hence

$$\frac{d\Delta}{d\ell} = -d\Delta + O(t,\lambda). \tag{45}$$

Therefore, this generated random coupling is irrelevant. Similar arguments apply for the variances of all the other random terms which are generated in the renormalization procedure.

We now follow standard procedures, and use an infinitesimal length rescale factor $b = e^{\delta\ell}$. To linear order in $\epsilon = d-2$, t and λ, equations (35, 40) now become

$$\frac{d}{d\ell}\frac{1}{t} = \epsilon\frac{1}{t} + \frac{2-\mathcal{N}}{2\pi} + \frac{1-\mathcal{N}}{2\pi}\frac{\lambda}{t},$$
$$\frac{d}{d\ell}\frac{\lambda}{t^2} = \epsilon\frac{\lambda}{t^2} + \frac{1-\mathcal{N}}{2\pi}\frac{\lambda}{t} + \frac{2-\mathcal{N}}{2\pi}\frac{\lambda^2}{t^2}. \tag{46}$$

Combining these two equations yields

$$\frac{dt}{d\ell} = -\epsilon t + \frac{\mathcal{N}-2}{2\pi}t^2 + \frac{\mathcal{N}-1}{2\pi}t\lambda,$$
$$\frac{d\lambda}{d\ell} = -\epsilon\lambda + \frac{\mathcal{N}-3}{2\pi}\lambda t + \frac{\mathcal{N}}{2\pi}\lambda^2. \tag{47}$$

Clearly, these equations show that $d = 2$ is the lower critical dimension for the NLσM with quenched dipoles. Hence, the 2D problem is exactly renormalizable (as done in the next section), and one can obtain an ϵ-expansion in $d = 2+\epsilon$ dimensions (as done in Appendix B).

4 The correlation length of a 2D Heisenberg system

We now proceed to calculate ξ_{2D}. To this end we solve equations (47) with the initial values $t(\ell_0) \equiv t_0$, and $\lambda(\ell_0) \equiv \lambda_0$. The parameter ℓ_0 represents some prefacing iterations. In the simplest case, we assume that $\ell_0 = 0$, and thus that $e^{\ell_0} \equiv L_0 = 1$. Other choices for L_0 will be discussed below. The solution is particularly simple for the Heisenberg system, $\mathcal{N} = 3$. At 2D one finds

$$\lambda(\ell) = \lambda_0\left(1-\frac{3\lambda_0}{2\pi}(\ell-\ell_0)\right)^{-1},$$
$$\frac{\lambda(\ell)}{t(\ell)} - 1 = \left(\frac{\lambda(\ell)}{\lambda_0}\right)^{1/3}\left(\frac{\lambda_0}{t_0}-1\right). \tag{48}$$

Both $t(\ell)$ and $\lambda(\ell)$ flow away from the fixed point $t = \lambda = 0$ as ℓ increases. From the second of equations (48) it is seen that $\lambda_0 > t_0$ implies $\lambda > t$, and *vice versa*.

The standard scaling relation for the correlation length is

$$\xi(t,\lambda) = e^{\ell}\xi(t(\ell),\lambda(\ell)). \tag{49}$$

The correlation length ξ is obtained from the matching condition at $\ell = \ell^*$,

$$\max\bigl(t(\ell^*),\lambda(\ell^*)\bigr) = 2\pi, \tag{50}$$

where ℓ^* is chosen so that $\xi(t(\ell^*),\lambda(\ell^*))$ is of the order of the renormalized lattice constant. In practice, this implies that at $\ell = \ell^*$, ξ is a slowly varying function of its variables, which we denote by $\tilde{C}(t,\lambda)$. The first of equations (48) gives

$$\ell^* - \ell_0 = \frac{2\pi}{3\lambda_0}\left(1 - \frac{\lambda_0}{\lambda(\ell^*)}\right), \tag{51}$$

where $\lambda(\ell^*)$ is equal to 2π for $\lambda_0 > t_0$, and is given by the solution of

$$\left(\frac{\lambda_0}{\lambda(\ell^*)}\right)^{2/3}\left[\left(\frac{\lambda_0}{\lambda(\ell^*)}\right)^{1/3} - 1 + \frac{\lambda_0}{t_0}\right] = \frac{\lambda_0}{2\pi}, \tag{52}$$

for $t_0 > \lambda_0$. Equations (49, 51) give the 2D correlation length,

$$\xi_{2D}(t,\lambda) = L_0\tilde{C}(t,\lambda)\exp\left[\frac{2\pi}{3\lambda_0}\left(1 - \frac{\lambda_0}{\lambda(\ell^*)}\right)\right]. \tag{53}$$

In the low temperature limit, $\lambda_0/t_0 \gg 1$, we stop iterating when $\lambda(\ell^*) = 2\pi$, and consequently

$$\xi_{2D} \approx L_0\tilde{C}(t,\lambda)\exp\left[\frac{2\pi}{3\lambda_0}\left(1 - \frac{\lambda_0}{2\pi}\right)\right]. \tag{54}$$

It follows that ξ_{2D} is finite at any finite λ_0, even as t_0 approaches zero. This implies that at zero temperature the long-range order in 2D Heisenberg magnets is destroyed at any small amount of defects (as indeed predicted already by Villain [1]). This conclusion is also supported by the observation mentioned above, that $\mathcal{H}_{int}$ represents correlated random fields. The exponential form of equation (54) is similar to that found for other random field problems at the lower critical dimension [11]. Monte-Carlo simulations [19] also suggest that the zero temperature correlation length is finite in 2D classical Heisenberg magnets with frustrated bonds. When the correlation length of the 2D system remains finite at zero temperature, it measures the size of the Imry-Ma domains, which is given by an exponential form like equation (54).

When $\lambda_0 < t_0 \ll 1$, we can approximate $\lambda_0/\lambda(\ell^*)$ by $(1-\lambda_0/t_0)^3$ (see Eq. (52)) and obtain

$$\xi_{2D} = L_0\tilde{C}(t,\lambda)\exp\left(\frac{2\pi}{t_0}\left[1 - \frac{\lambda_0}{t_0} + \frac{\lambda_0^2}{3t_0^2}\right]\right). \tag{55}$$

The exponential part may be interpreted as a renormalization of the effective stiffness constant in the usual expression for the 2D Heisenberg model,

$$\begin{aligned}\rho_s^{eff} &= \rho_s(1 - y + y^2/3),\\ y &= \lambda_0/t_0 = Ax\rho_s/T,\end{aligned} \tag{56}$$

where we have used equation (8). To leading order in $x\rho_s/T$, this coincides with the expression which was obtained in reference [3] for an annealed system of dipoles. Indeed, up to the lowest order in λ/t there is no difference between quenched and annealed averaging.

Finally, we discuss the pre-exponential factor in the expressions for the correlation length. For $\lambda_0 \ll t_0$, the prefactor $\tilde{C}(t,\lambda) \approx \tilde{C}(t_0,0)$ is known: The two-loop [9] and three-loop [20] calculations, based on the quantum NLσM, show that

$$\tilde{C}(t_0,0) = \frac{e}{8}\frac{c}{2\pi\rho_s}\left(1 - \frac{t_0}{4\pi}\right), \tag{57}$$

where c is the spin-wave velocity.

At low temperatures, we need the concentration dependence of the pre-exponential factor. This results from higher order loops: At 2D, $t = 0$ and $\mathcal{N} = 3$, the generalized recursion relation for λ has the generic form

$$\frac{d\lambda}{d\ell} = \beta_2\lambda^2 + \beta_3\lambda^3, \tag{58}$$

with $\beta_2 = 3/(2\pi)$ and with β_3 of order β_2^2. The solution for this equation reads

$$\begin{aligned}e^{\ell-\ell_0} = &\left(\frac{\lambda_0(\beta_2+\beta_3\lambda(\ell))}{\lambda(\ell)(\beta_2+\beta_3\lambda_0)}\right)^{\beta_3/\beta_2^2}\\ &\times\exp\left[\frac{1}{\beta_2}\left(\frac{1}{\lambda_0} - \frac{1}{\lambda(\ell)}\right)\right],\end{aligned} \tag{59}$$

and therefore, at $\ell = \ell^*$, where $\lambda(\ell^*) = 2\pi$, we have $e^{\ell^*} \sim L_0 x^{\beta_3/\beta_2^2}\exp[2\pi/(3\lambda_0)]$. Consequently, $\tilde{C}(t,\lambda) \approx \tilde{C}(0,\lambda) \approx C_0\lambda^{\omega}$, with $\omega = \beta_3/\beta_2^2$.

Within the approximations leading to equations (54, 55), we note that the expressions in the exponentials and their first derivatives are continuous at $\lambda_0 = t_0$, up to terms of order $\mathcal{O}(\lambda_0/2\pi)$. In comparing our results with the experiment, we shall use these asymptotic expressions all the way to the line $\lambda_0 = t_0$.

5 The phase boundary for weakly coupled planes

The 3D transition temperature $T_N(x)$, as function of the defect concentration x, of a system consisting of weakly coupled planes may be deduced from the relation

$$\alpha\xi_{2D}^2(t_N,\lambda) \sim 1. \tag{60}$$

(Note that λ is proportional to x, *cf.* Eq. (8).) The parameter α can be generated by an interplane exchange, $J_\perp/J \sim J_\perp/2\pi\rho_s$, or some in-plane spin anisotropy. As stated in the Introduction, this procedure gives excellent estimates for T_N [10].

To obtain the critical line $T_N(x)$ we proceed as follows. Using (53) in the relation (60) we find

$$1 - \frac{\lambda_0}{\lambda(\ell^*)} = \frac{3\lambda_0}{4\pi}\ln\bigl[\alpha\bigl(L_0\tilde{C}(t,\lambda)\bigr)^2\bigr]^{-1}. \tag{61}$$

At low temperature, *i.e.*, for $\lambda_0 > t_0$, we have $\lambda(\ell^*) = 2\pi$ and therefore equation (61) is almost independent of t. It thus yields a critical value for the initial value of the variance, λ_c, and hence a critical concentration, x_c, above which there is no antiferromagnetic long-range order at any temperature

$$\lambda_c = \frac{2\pi}{1 + \frac{3}{2}\ln\left[\alpha\left(L_0\tilde{C}(0,\lambda_c)\right)^2\right]^{-1}}, \tag{62}$$

with $\lambda_c = Ax_c$. In fact, ξ_{2D} is expected to be practically independent of temperature (except for the very weak dependence of the prefactor $\tilde{C}$) for a range of values, $\lambda_0 > t_0$, as given in equation (54). Therefore, the critical line $T_N(x)$ is expected to be practically vertical for $t_N(x) < \lambda_0 = Ax$. Below this line, one might expect some range in which spin glass and antiferromagnetism co-exist, down to a Gabay-Toulouse like line [6]. To obtain this region one would need to also consider the 3D boundaries of the spin glass phase, as well as the anisotropies which allow the existence of spin glass long range order, and this is beyond the scope of the present paper. In any case, the AFM ordering will persist up to the line $x = x_c$.

At smaller defect concentrations, or at higher temperatures, *i.e.*, for $2\pi \gg t_0 > \lambda_0$, equations (52, 61) give

$$1 - \frac{\lambda_0}{t_N(x)} = \left\{1 - \frac{3\lambda_0}{t_N(0)}\right\}^{1/3},$$
$$\frac{1}{t_N(0)} = \frac{1}{4\pi}\ln\left[\alpha\left(L_0\tilde{C}(t_N(0),0)\right)^2\right]^{-1}, \tag{63}$$

where $t_N(0)$ is the Néel temperature of the pure antiferromagnet. The lowest order of this expression agrees with the results of reference [3], obtained by an annealed average.

6 Annealed averaging

As stated above, the description of FM bonds in an antiferromagnet by dipoles requires some mixed annealed-quenched averaging. We start by reviewing a simple version of GI's analysis [3]. In their approach, $\mathbf{r}_\ell$ and $\mathbf{a}(\mathbf{r}_\ell)$ are treated as quenched variables, with averages given by equation (6), while $\mathbf{m}(\mathbf{r}_\ell)$ is treated as annealed. Thus, equation (7) is replaced by

$$[f_{i\mu}(\mathbf{r}_1)f_{j\nu}(\mathbf{r}_2)] = \delta_{ij}\delta(\mathbf{r}_{12})\Lambda_{\mu\nu}(\mathbf{r}_1), \tag{64}$$

with

$$\Lambda_{\mu\nu}(\mathbf{r}) = m_\mu(\mathbf{r})m_\nu(\mathbf{r})M^2x/d. \tag{65}$$

Initially, $\mathcal{H}$ contains no interactions among the dipole moments $\{\mathbf{m}(\mathbf{r})\}$. However, the RG iterations generate the dipole-dipole interaction, as given by equation (29). This interaction is mediated via the canted background AFM moments. Treating this interaction as a small perturbation, to lowest order, we can next integrate the dipole moments out of the partition function, using the annealed averaging $\langle m_\mu(\mathbf{r}_1)m_\nu(\mathbf{r}_2)\rangle = \delta_{\mu\nu}\delta(\mathbf{r}_{12})/\mathcal{N}$, so that

$$\langle\Lambda_{\mu\nu}\rangle = \delta_{\mu\nu}\Lambda \equiv \delta_{\mu\nu}M^2x/(d\mathcal{N}). \tag{66}$$

Note that to this leading order, $\Lambda = \lambda$! GI wrote down a more general form for this thermal average, involving the susceptibility which results from the quadratic coupling in $\mathcal{H}_{dd}$. This reduces to the above expression at lowest order.

Up to equation (33), we have performed no averaging. In the annealed case, the recursion relation are derived from the same equations, using the averages as listed above. The resulting recursion relation for $1/t$ turns out to be the same as equation (35), with λ replaced by Λ. In contrast, the averaging over $\mathbf{m}$ gives no contributions to the renormalization of $\mathbf{f}_i$, since all the generated terms which are linear in B_i^μ involve odd powers of the u_i's and the g_i^μ's, and therefore odd powers of the m_μ's. All of these vanish upon the annealed averaging over the m_μ's. Thus, we end up with

$$\left(\frac{\Lambda}{t^2}\right)' = b^{d-2}\left(\frac{\Lambda}{t^2}\right). \tag{67}$$

At 2D, equation (67) implies that Λ is unrenormalized. The solution of the recursion relation for t then yields

$$\ell = \frac{\pi}{\Lambda}\ln\frac{1 + 2\Lambda/t(0)}{1 + 2\Lambda/t(\ell)}. \tag{68}$$

Assuming that $\Lambda \ll 2\pi$, and integrating up to $t(\ell^*) = 2\pi$, yields

$$\ell^* \approx \frac{2\pi}{t(0)}\left(1 - \frac{\Lambda}{t(0)}\right), \tag{69}$$

which agrees to leading order with the quenched result (55).

This annealed averaging is legitimate as long as the renormalized distance between the impurities remains large, so that the dipole-dipole interaction which is generated during the iterations remains small. Note that the range of $\mathcal{H}_{dd}$ is $b = e^{\ell^*}$. Thus, if e^{ℓ^*} is small compared to the inter-impurity distance $x^{-1/d}$, then we can still treat the dipoles as independent degrees of freedom, ignore the interaction between them and continue the above annealed calculation. However, if e^{ℓ^*} becomes larger than (but of the order of) $x^{-1/d}$ then each renormalized cell contains more than one impurity, and the interaction between them comes into play. Since this interaction decays as $1/r^d$, the dipoles behave like a spin glass which is at its lower critical dimension [6]. We thus expect the dipole moments to develop spin-glassy correlations, with a correlation length ξ_{sg} which grows exponentially in E_{dd}/T, where $E_{dd} = \lambda\rho_s$ represents the dipole-dipole energy. Having shown that ξ_{2D} remains finite at all T, we expect that for $T \ll E_{dd}$ one has $\xi_{sg} \gg \xi_{2D}$, the moments inside a renormalized cell (at distances smaller than ξ_{2D}) freeze randomly, with the effective Edwards-Anderson order parameter Q, and we can switch to our quenched calculation.

We thus choose to perform a prefacing annealed renormalization, up to $e^{\ell_0} = L_0 \sim x^{-1/d}$. For larger ℓ we assume that the dipole moments are frozen at low T, and we switch to the quenched analysis of Sections 4 and 5.

7 Comparison with experiments on doped cuprates

One motivation of the present study arises from its possible relevance to the understanding of the doping dependence of the magnetic order in the lamellar copper oxides. Experimentally, doping such oxides leads to a rapid decrease in both ξ_{2D} and T_N [10,21–27]. Experiments on doped La_2CuO_4 show that above $x = x_c \approx 2\%$, ξ_{2D} remains finite even at zero temperature, and there is no AFM order. This strong effect of the doping has been attributed to frustration, because of the strong FM exchange on the Cu–O–Cu bonds which (at small x) have localized holes due to the doping [7]. This frustration also led to the prediction of a magnetic spin glass phase for $x > x_c$ [7], as recently confirmed in detail in doped La_2CuO_4 [28]. The experimental verification of this spin freezing above x_c [10,25,27–30] confirms the picture of *localized* holes. This localization is also confirmed by direct conductance measurements at $x \leq 5\%$ and low temperature T [10,29].

Although the above picture may not be the only possible explanation for the phase diagram of the cuprates at low x, the following discussion assumes the frustration model and then shows that the experiments are consistent with the predictions of the previous sections. As stated above, the most direct application of our theory is at zero temperature, where our quenched averaging should apply. In that limit we use the results from Sections 4 and 5. The other limit, of low x, is also easy: then the quenched and annealed averages coincide, and to linear order in x we can compare experiments with the GI result, based on equation (68). Although there exist uncertainties on where exactly one should switch from quenched to annealed averaging, we fit the experiments to the expressions which follow from our quenched calculation. These expressions are correct in *both* limits of low x and low T, and should thus supply a good interpolation for the whole range near the 3D transition temperature $T_N(x)$.

For the fitting, we adopt the following strategy: We start by fitting $A \equiv \lambda/x$ from the t-dependence of ξ_{2D} at high T and small x. As stated, this dependence is the same for both types of averages, and could already be done using the results of GI. Given A, we next fit the x dependence of ξ_{2D} in the limit of very low T, when ξ_{2D} is T-independent. This behavior should be described by our quenched theory. The fit determines the pre-exponential factors. Finally, we use the results (without any further adjustments) to calculate the phase diagram, $T_N(x)$. This calculation is based on our quenched formulation, and thus involves some interpolation.

We begin with the temperature dependence of the correlation length at low concentrations, $x < x_c$. Data taken on a sample of $La_2CuO_{4+\delta}$, with $T_N = 90$ K [10], show a practically linear dependence of $(t/2\pi)\ln(\xi/C)$ on $1/t$, in agreement with both our quenched result (55) and our annealed result (69). For the coefficient C in this fit we used $C = 1.92$ Å, derived from equation (57) with $\rho_s = 24$ meV (See Ref. [10]) and $L_0 = 1$. The slope is $\Lambda = \lambda_0 = 0.29(1)$ (see Fig. 1, and also Ref. [4]). To estimate the value of x for this sample, we follow references [10,31] and approximate the line $T_N(x)$ by the straight line $T_N(x) \approx 325 - 16250x$, which extrapolates to $x = 0.02$ as T_N is extrapolated to zero. Using this approximation, we find that $T_N = 90$ K at $x = 0.0145$. Thus, $A = \lambda/x \approx 20$. Although we have some problems with this linear extrapolation (see below), the value of x cannot be larger than $x_c \approx 0.02$, so the uncertainty in A is not more than 30%. Furthermore, although A might have a weak dependence on T and on x, this could most probably be absorbed in this error estimate. We thus use this estimate $A = 20$ in everything that follows.

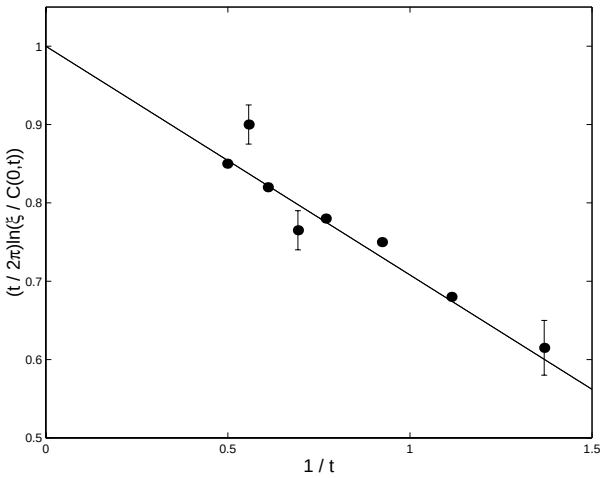

Fig. 1. $(t/2\pi)\ln(\xi/C)$ *versus* $1/t$ for $La_2CuO_{4+\delta}$ with $T_N = 90$ K. The points are from reference [10]. The straight line shows the fit to equation (55), with $\lambda_0/t_0 \ll 1$.

Keimer *et al.* [10] measured the temperature dependence of the correlation length for three magnetically disordered samples of $La_{2-x}Sr_xCuO_4$, with $x \approx 0.02$, 0.03, and 0.04. The error in x is less than ~ 0.005. It is believed [10] that the hole concentration is about that of the Sr ions. It was found that at low temperatures ξ does not depend on T, and falls with the increase of x faster than a power law. The $\xi(T = 0)$ data is depicted in Figure 2, together with the value of ξ cited in reference [29] for $La_{1.95}Ba_{0.05}CuO_4$. The figure also shows the theoretical values of ξ, calculated from equation (54), with $L_0\tilde{C}(0,\lambda_0) = C_0\lambda_0^{\omega'}$, $\lambda_0 = 20\,x$, $C_0 = 2.8$ Å and $\omega' = 0.8$. (In 2D, we now have $\omega' = \omega - 1/2$, from the x dependence of L_0.) We also reproduce in Figure 2 the numerical results obtained in reference [19]. These authors computed the effect of holes localized on the oxygen atoms in the CuO_2 plane. Their results, marked by "+" in Figure 2, are in agreement with our calculation.

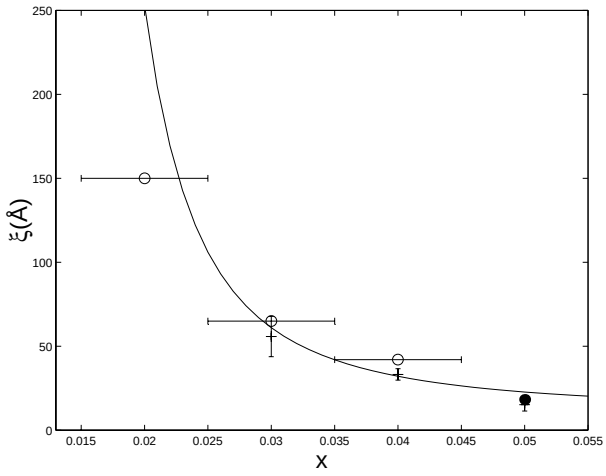

Fig. 2. Dependence of ξ_{2D} at $T = 0$ on x. The empty [10] and full [29] circles indicate experiments, +'s show numerical simulation [19] data. The solid line represents $2.8\lambda^{0.8}$ Å $\exp(2\pi/3\lambda)$, with $\lambda = 20x$.

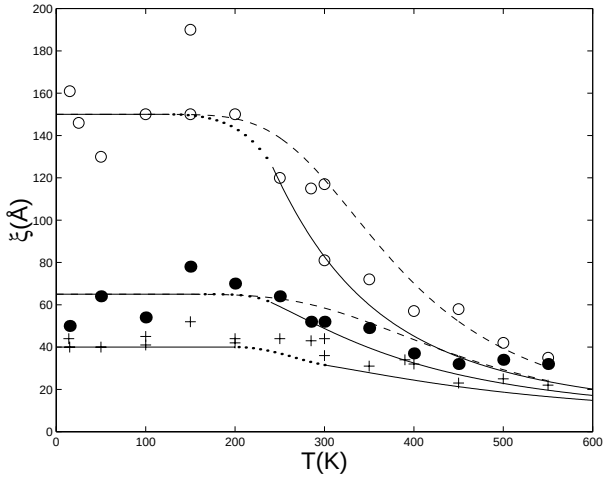

Fig. 3. Dependence of $\xi_{2D}(t, \lambda)$ on T for several concentrations. Symbols are from experiments: empty circles for $x = 0.02$, full circles for $x = 0.03$, +'s for $x = 0.04$, all from reference [10]. Full lines show results from Figure 2 (for low T) or equation (55), with $C = L_0\tilde{C} = 1.92$ Å (for high T). Dotted lines interpolate between these low- and high-T theories. Dashed lines correspond to equation (70).

We next turn to the temperature dependence of ξ at $x > x_c$. Figure 3 exhibits the calculated temperature dependence of ξ, for several concentrations x. The curves were found from equation (55) with $C = L_0\tilde{C} = 1.92$ Å ($\lambda_0 < t_0$, as in Figure 1 discussed above), and from equation (54), with $C(x) = 2.8\lambda_0^{0.8}$ Å ($\lambda_0 > t_0$). We have also used $2\pi\rho_s = 150$ meV. The theoretical lines are for $x = 0.0225$, 0.029 and 0.036 (instead of the experimental values 0.02, 0.03, and 0.04 given by Keimer *et al.*). The values chosen are within the experimental error [10]. Since the prefactors used in our fits differ in the limits $\lambda_0 \ll t_0$ and $\lambda_0 \gg t_0$, the high- and low-temperature portions of the plots do not match at $\lambda_0 = t_0$. There the two segments are connected by dotted lines. This intermediate region is in any case outside the scope of our theory. The dashed lines in Figure 3 represent the heuristic expression

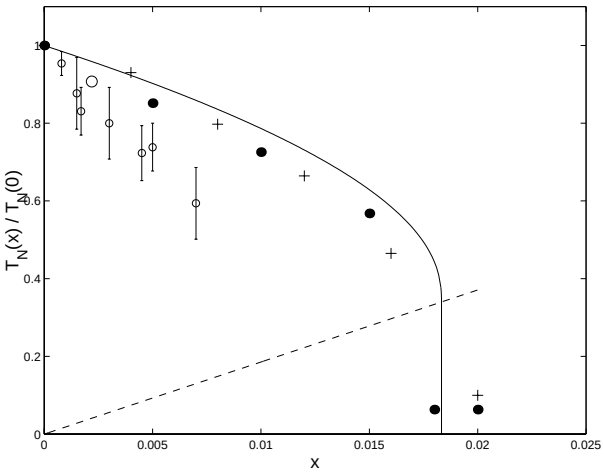

Fig. 4. $T_N(x)/T_N(0)$ *versus* x. Full line is theory, and the points are from experiments: full circles from reference [23], +'s from reference [24], empty circles from references [31,32]. Dashed line indicates $\lambda_0 = t_0$.

$$\xi^{-1}(T, x) = \xi^{-1}(0, x) + \xi^{-1}(T, 0), \tag{70}$$

used in reference [10] to fit their data. It seems that the heuristic expression works as well; however, it seems that it has no theoretical basis.

The theoretical curves in Figure 3 agree with the experimental results at temperatures lower than $\sim 350-400$ K. At higher temperatures the calculated values of ξ are smaller than the measured ones. Perhaps, at such high temperatures thermal fluctuations come into play, causing a decrease of Q from $1/\mathcal{N}$ to lower values. It is also possible that at high T the holes are more mobile, so that one should average over more than one bond per hole, thus reducing the effective dipole moment. At temperatures lower than $200-250$ K the correlation length does not depend on the temperature up to exponentially small terms, of the order of $\xi(0, T)^{-1}$ [10]. This nontrivial property of the correlation length is reproduced well by our calculation.

Given the above values for C_0 and ω, and the value $\alpha = 10^{-4}$ from reference [10], we solved equation (62) and found the critical value of λ to be $\lambda_c = 0.366$. With $A = 20$, the critical concentration, x_c, for the disappearance of the long-range order at $T = 0$ is found to be $x_c = 0.0183$, in very good agreement with the experimental value $x_c = 0.0175$ from reference [22] (but in disagreement with Ref. [26], which gives $x_c = 0.027$).

Using the above parameters, *i.e.* $A = 20$, $\alpha = 10^{-4}$, and approximating the prefactor by a constant, $C(t, x) \approx C(0, x_c) = C(0, 0.0183) = 1.26$ Å, Figure 4 shows the theoretical concentration dependence of T_N, calculated from

equations (63) for $t_0 > \lambda_0$ and (62) for $\lambda_0 > t_0$, with no further fitting of the parameters. (The line $t_0 = \lambda_0$ is also depicted in the figure.) At high temperatures the prefactor is larger, 1.9 Å. However, the effect of this difference on T_N is small, since T_N depends on the prefactor only logarithmically. At small concentrations, our theoretical $T_N(x)$ decreases with the increase of x linearly with the rate 55 K/% (based on the value of A as determined from the ξ data). At $x = x_c$, $T_N(x_c)$ is roughly equal to $T_N(0)/3$. Then T_N abruptly falls to zero, as our calculation finds that the correlation length is independent of the temperature for $t_0 < \lambda_0$.

Figure 4 includes the results of several experiments. It is seen that those of reference [31] seem to disagree with our phase diagram: the data fall linearly with a slope of 162 K/%, (larger by about a factor of 3 than our theoretical value, which was extracted from the data for ξ), extrapolating to $x = 0.02$ without the jump in T_N. However, we should note that Chen *et al.* [31] determined x for their O-doped samples from Hall effect data. In reference [32] T_N and the Hall density of holes were measured for a Sr doped sample. The Sr concentration in the melt was 0.0022, while the Hall measurements gave a smaller hole density, 0.0016. Figure 4 shows that in this case the experimental point (with $x = 0.0022$) is closer to the theoretical curve than the data from reference [31]. Saylor and Hohenemser [23] measured $T_N(x)$ in Sr-doped samples of lanthanum cuprate. Although their $T_N(0) = 317$ K was somewhat less than in the best samples of reference [10], their $T_N(x)$ decreased linearly with the rate 90 K/% till $x = 0.015$. In the region between $x = 0.015$ and 0.018, T_N fell from ≈ 180 K to 20 K. This behavior of $T_N(x)$ is close to our phase diagram, Figure 4.

Very recently, Wakimoto *et al.* [27] measured the phase diagram of oxygen doped $La_{1.95}Bi_{0.05}CuO_4$, and their $T_N(x)$ agrees qualitatively with our theory: it falls almost linearly down to $T_N(0.012) \approx 160$ K, and then drops sharply towards $x_c \approx 0.015$. Both this small value of x_c and the low-T value of the correlation length near x_c, as measured in reference [27], are consistent with our calculations, with $A \approx 30$.

8 Conclusions

Most of this paper was devoted to a detailed description of the theory for the effects of quenched dipolar defects on AFM correlations in doped antiferromagnets. The results should apply directly to problems with correlated random fields, and could generate future expansions in $(2 - \theta)$ for related problems. A second major part of the paper was devoted to the effects of quenched FM bonds in an antiferromagnet. This required some discussion of quenched-annealed averaging and interpolation between the two types of averaging. We hope that this discussion will stimulate some further studies of such systems, *e.g.* by numerical simulations or by theories which would cover the intermediate temperature and concentration regime. We also hope that our study will stimulate more material research onto AFM-FM mixed systems.

In the previous section we discussed some fits of our theory (using the results for quenched averaging) to data from doped lamellar oxides. As stated, these fits are based on various assumptions. However, we find it satisfactory that our theory reproduces many of the features observed in these experiments.

Before concluding, we would like to note that dipolar defects of the kind discussed in our paper may arise not only from single FM bonds; they will also arise from larger finite localized defects, provided these defects prefer a local FM ordering of the spins. Therefore, our results may also apply to the cuprates even if the localization length of the holes there is larger than one. Indeed, experiments indicate a localization length of a few lattice constants [31,32]. A similar dipole-like decay of the canted moments, as $1/r$, was also predicted for the case when the holes are localized around the center of a Cu plaquette in the plane, instead of the oxygen ion [33]. Our results may thus also apply to that case.

Finally, we note that the calculation presented above ignored quantum spin fluctuations. We have checked that integration of the quantum fluctuations, similar to that done in reference [9], only renormalizes the initial parameters of the effective classical model also in the random case. Therefore, our theory also applies for the quantum case at finite temperatures.

We have benefitted from many discussions with R.J. Birgeneau, A.B. Harris, A.S. Ioselevich, M.A. Kastner, D.E. Khmel'nitskii, V.V. Lebedev, T. Nattermann and M. Schwartz. This project has been supported by a grant from the U. S.-Israel Binational Science Foundation (BSF) and from the Israel Science Foundation.

Appendix A: Gauge transformation of the fields ϕ_μ

In order to eliminate the functions $A_i^{\mu\nu}(\mathbf{r})$ from the expression for the derivatives $\partial_i \tilde{\mathbf{n}}$ (Eq. (16)) we introduce the transformation

$$\phi_\mu = \sum_{\mu_1} T_{\mu\mu_1} \tilde{\phi}_{\mu_1}, \tag{A.1}$$

where the coefficients $T_{\mu\mu_1}$ are determined by

$$\partial_i T_{\mu\mu_1} = \sum_{\mu_2} A_i^{\mu\mu_2} T_{\mu_2\mu_1}, \tag{A.2}$$

with

$$\sum_{\mu} T_{\mu\mu_1} T_{\mu\mu_2} = \delta_{\mu_1\mu_2}, \quad T_{\mu\mu_1} = T_{\mu_1\mu}. \tag{A.3}$$

Note that the sums run from 1 to $\mathcal{N} - 1$. Assuming that $A_i^{\mu\mu_1}$ is independent of x_i, the solution of equations (A.2, A.3) reads $T_{\mu\mu_1} = T^0_{\mu\mu_1} \exp(-i\kappa x_i)$, where κ is a real eigenvalue of the Hermitian matrix iA_i. Deviations from this approximation naturally involve higher derivatives of

$A_i^{\mu\mu_1}$ which are related to higher powers of the gradients in $\mathcal{H}$. These are strongly irrelevant.

Inserting the above relations into equation (16) we obtain

$$\partial_i \mathbf{n} = \tilde{\mathbf{n}} \left[\partial_i \sqrt{1-\tilde{\phi}^2} - \sum_\mu \tilde{\phi}_\mu \sum_\nu T_{\nu\mu} B_i^\nu \right] + \sum_\mu \left[B_i^\mu \mathbf{e}_\mu \sqrt{1-\tilde{\phi}^2} + \partial_i \tilde{\phi}_\mu \sum_\nu T_{\nu\mu} \mathbf{e}_\nu \right]. \quad \text{(A.4)}$$

Therefore, defining

$$\tilde{\mathbf{e}}_\mu = \sum_\nu \mathbf{e}_\nu T_{\nu\mu}, \quad \tilde{B}_i^\mu = \sum_\nu B_i^\nu T_{\nu\mu}, \quad \text{(A.5)}$$

Equation (A.4) takes the form of equation (16) without the $A_i^{\nu\mu}$ terms, with ϕ_μ, $\mathbf{e}_\mu$ and B_i^μ replaced by $\tilde{\phi}_\mu$, $\tilde{\mathbf{e}}_\mu$ and $\tilde{B}_i^\mu$, respectively. For brevity, we have omitted in the subsequent derivations the superscript $\tilde{}$. It is seen that the gauge transformation can be regarded as a rotation of the base vectors $\mathbf{e}_\mu$, and reflects the arbitrariness of their choice [16].

Appendix B: The phase boundary at $2+\epsilon$ dimensions

For completeness, we present here the solution of the recursion relations (47) in $d = 2+\epsilon$ dimensions, and obtain the critical line $t_N(x)$, where x is the defect concentration.

The recursion relations (47) have four fixed points in the $[\lambda, t]$ plane: $[0,0]$, $[0, 2\pi\epsilon/(\mathcal{N}-2)]$, $[2\pi\epsilon/\mathcal{N}, 0]$, and $[2\pi\epsilon/(2\mathcal{N}-3), 2\pi\epsilon/(2\mathcal{N}-3)]$. For $\mathcal{N} > 3/2$, the first point is stable, the last one is doubly unstable and the other two are unstable in one direction and stable in the other.

The solution of equations (47) for $\ell > \ell_0$ and Heisenberg spins ($\mathcal{N} = 3$) reads

$$\lambda(\ell) = \lambda_0 \left[e^{\epsilon(\ell-\ell_0)} - \frac{3\lambda_0}{2\pi\epsilon}\left(e^{\epsilon(\ell-\ell_0)} - 1\right) \right]^{-1},$$
$$\frac{1-\lambda(\ell)/t(\ell)}{1-\lambda_0/t_0} = \left[\frac{\lambda(\ell) - 2\pi\epsilon/3}{\lambda_0 - 2\pi\epsilon/3} \right]^{1/3}. \quad \text{(B.1)}$$

The phase boundary is identified as the line which separates the flow to the origin (in the ordered phase) from the flow to infinity (in the disordered phase). It is easy to check that for $t_0 > \lambda_0$, the initial point $[\lambda_0, t_0]$ will flow to the "pure" fixed point $[0, 2\pi\epsilon]$ when

$$1 - \frac{\lambda_0}{t_N(x)} = \left(1 - \frac{3\lambda_0}{2\pi\epsilon}\right)^{1/3},$$
$$0 \le \lambda_0 \le \lambda_c = \frac{2\pi\epsilon}{3}, \quad \text{(B.2)}$$

where the second of equations (B.1) has been used. On the other hand, using again that equation, we find that for $t_0 < \lambda_0$ the solution flows to the "random" fixed point, $[2\pi\epsilon/3, 0]$, provided that

$$\lambda_0 \equiv \lambda_c = \frac{2\pi\epsilon}{3}, \quad \lambda_c > t_0 > 0. \quad \text{(B.3)}$$

The two portions of the critical line, equations (B.2, B.3), are separated by the multicritical point at $[2\pi\epsilon/3, 2\pi\epsilon/3]$. It is interesting to note that also here, like the behavior found for $t_N(x)$ for weakly coupled planes, there is a vertical section of the phase boundary.

We thus conclude that for $t_0 > \lambda_0$ the randomness is irrelevant, and the "pure" critical behavior (which has a correlation length exponent $\nu = 1/\epsilon$) remains stable. However, finite values of λ yield a correction to this behavior, with exponent $-\epsilon$ (or, more generally, $-\epsilon/(\mathcal{N}-2)$). The correlation length is obtained from equation (49), using the matching conditions (50). One finds

$$\xi \sim \exp(\ell^*) = L_0 \left[\frac{\lambda^{-1}(\ell^*) - \lambda_c^{-1}}{\lambda_0^{-1} - \lambda_c^{-1}} \right]^{1/\epsilon}. \quad \text{(B.4)}$$

For $t_0 > \lambda_0$ the iterations are stopped at $t(\ell^*) \sim 2\pi$. In the range $\lambda(\ell^*) < \lambda_c$ we can find $\lambda(\ell^*)$ by considering the difference $\lambda_0/t_N - \lambda_0/t_0$, using equations (B.1, B.2). We find

$$t_N^{-1} - t_0^{-1} \simeq \lambda_0^{-1} \frac{\lambda(\ell^*)}{3\lambda_c} \left(1 - \frac{\lambda_0}{\lambda_c}\right)^{1/3}, \quad \text{(B.5)}$$

from which it follows that

$$\xi \sim e^{\ell^*} \sim (t_0 - t_N(x))^{-1/\epsilon} [1 + Bx(t_0 - t_N(x)) + ...], \quad \text{(B.6)}$$

where B is a constant and the term associated with it comes from corrections of order $\lambda_0 e^{-\ell^*}$. For $\lambda_0 > t_0$, $\lambda(\ell^*) = 2\pi$, so that

$$\xi \sim e^{\ell^*} \sim (\lambda_0^{-1} - \lambda_c^{-1})^{-1/\epsilon}. \quad \text{(B.7)}$$

Note added in proofs

Recently, M. Hücker *et al.* (Phys. Rev. B **59**, R725 (1999)) published new data for $T_N(x)$ in $La_{1-x}Sr_xCuO_4$. These data fully agree with our phase diagram, Figure 4. The slope of $T_N(x)$ at small x also confirms our estimate of the parameter A.

References

1. J. Villain, Z. Phys. B **33**, 31 (1979).
2. J. Vannimenus, S. Kirkpatrick, F.D.M. Haldane, C. Jayaprakash, Phys. Rev. B **39**, 4634 (1989); P. Gawiec, D.R. Grempel, Phys. Rev. B **44**, 2613 (1991).
3. L.I. Glazman, A.S. Ioselevich, Z. Phys. B **80**, 133 (1990).
4. I.Ya. Korenblit, Phys. Rev. B **51**, 12 551 (1995).
5. K. Binder, A.P. Young, Rev. Mod. Phys. **58**, 80 (1986).

6. K.H. Fischer, J.A. Hertz, *Spin Glasses* (Cambrige University Press, 1991).
7. A. Aharony, R.J. Birgeneau, A. Coniglio, M.A. Kastner, H.E. Stanley, Phys. Rev. Lett. **60**, 1330 (1988).
8. P. Lacour-Gayet, G. Toulouse, J. Phys. France **35**, 425 (1974).
9. S. Chakravarty, B.I. Halperin, D.R. Nelson, Phys. Rev. B **39**, 2344 (1989).
10. *e.g.* B. Keimer, N. Belk, R.J. Birgeneau, A. Cassanho, C.Y. Chen, M. Greven, M.A. Kastner, A. Aharony, Y. Endoh, R.W. Erwin, G. Shirane, Phys. Rev. B **46**, 14 034 (1992).
11. Y. Imry, S.K. Ma, Phys. Rev. Lett. **35**, 1399 (1975).
12. E. Brézin, J. Zinn-Justin, Phys. Rev. B **14**, 3110 (1976).
13. D.R. Nelson, R.A. Pelcovits, Phys. Rev. B **16**, 2191 (1977).
14. D.S. Fisher, Phys. Rev. B **31**, 7233 (1985).
15. M. Schwartz, J. Villain, Y. Shapir, T. Nattermann, Phys. Rev. B **48**, 3095 (1993).
16. A.M. Polyakov, Phys. Lett. B **59**, 79 (1975); Gauge Fields and Strings, in *Contemporary Concepts in Physics*, edited by H. Feshbach (Harwood Academic, 1987).
17. V.L. Berezinskii, A. Ya. Blank, Sov. Phys. JETP **37**, 369 (1973).
18. A.Z. Patashinskii, V.L. Pokrovskii, *Fluctuation Theory of Phase Transitions* (Pergamon Press, Oxford, 1979).
19. R.J. Gooding, A. Mailhot, Phys. Rev. B **44**, 11 852 (1991).
20. P. Hasenfranz, F. Nidermayer, Phys. Lett. B **268**, 231 (1991).
21. R.J. Birgeneau, G. Shirane, in *Physical Properties of High Temperature Superconductors*, edited by D.M. Ginzberg (World Scientific, Singapore, 1989).
22. G. Shirane, R.J. Birgeneau, Y. Endoh, M.A. Kastner, Physica B **197**, 158 (1994).
23. J. Saylor, C. Hohenemser, Phys. Rev. Lett. **22**, 1824 (1990).
24. J.H. Cho, F.C. Chou, D.C. Johnston, Phys. Rev. Lett. **70**, 222 (1993).
25. F.C. Chou, F. Borsa, J.H. Cho, D.C. Johnston, A. Lascialfari, D.R. Torgeson, J. Ziolo, Phys. Rev. Lett. **71**, 2323 (1993).
26. H. Kageyama, K. Yoshimura, M. Kato, K. Kosuge, J. Phys. Soc. Jpn **64**, 2144 (1995).
27. S. Wakimoto, K. Kurahashi, C.H. Lee, K. Yamada, Y. Endoh, S. Hosoya, Physica B **237-238**, 91 (1997).
28. F.C. Chou, N.R. Belk, M.A. Kastner, R.J. Birgeneau, A. Aharony, Phys. Rev. Lett. **75**, 2204 (1995) and references therein.
29. S.H. Hayden, G. Appeli, H. Mook, D. Rytz, M.F. Hundley, Z. Fisk, Phys. Rev. Lett. **66**, 821 (1991).
30. Ch. Niedermayer, C. Bernhard, T. Blasius, A. Golnik, A. Moodenbaugh, J.I. Budnick, Phys. Rev. Lett. **80**, 3843 (1998).
31. C.Y. Chen, R.J. Birgeneau, M.A. Kastner, N.W. Preyer, T. Thio, Phys. Rev. B **43**, 392 (1991).
32. C.Y. Chen, E.C. Branlund, ChinSung Bae, K. Yang, M.A. Kastner, A. Cassanho, R.J. Birgeneau, Phys. Rev. B **51**, 3671 (1995).
33. B. Shraiman, E.D. Siggia, Phys. Rev. B **42**, 2485 (1990). See also V.L. Pokrovsky, G.V. Uimin, Physica C **160**, 323 (1989); R.J. Gooding, Phys. Rev. Lett. **66**, 2266 (1991); R.J. Gooding, N.M. Salem, A. Mailhot, Phys. Rev. B **49**, 6067 (1994); R.J. Gooding, A. Mailhot, Phys. Rev. B **48**, 6132 (1993).